



SyntEyes KTC: higher order statistical eye model for developing keratoconus

Jos J. Rozema^{1,2}, Pablo Rodriguez³, Irene Ruiz Hidalgo^{1,2}, Rafael Navarro³, Marie-José Tassignon^{1,2} and Carina Koppen^{1,2}

¹Department of Ophthalmology, Antwerp University Hospital, Edegem, Belgium, ²Department of Medicine and Health Sciences, Antwerp University, Wilrijk, Belgium, and ³Facultad de Ciencias, ICMA, Consejo Superior de Investigaciones Científicas & Universidad de Zaragoza, Zaragoza, Spain

Citation information: Rozema JJ, Rodriguez P, Ruiz Hidalgo I, Navarro R, Tassignon MJ & Koppen C. SyntEyes KTC: higher order statistical eye model for developing keratoconus. *Ophthalmic Physiol Opt* 2017. doi: 10.1111/opo.12369

Keywords: keratoconus, ocular biometry, statistical eye model

Correspondence: Jos J Rozema
E-mail address: jos.rozema@uza.be

Received: 14 October 2016; Accepted:
7 February 2017

Abstract

Purpose: To present and validate a stochastic eye model for developing keratoconus to e.g. improve optical corrective strategies. This could be particularly useful for researchers that do not have access to original keratoconic data.

Methods: The Scheimpflug tomography, ocular biometry and wavefront of 145 keratoconic right eyes were collected. These data were processed using principal component analysis for parameter reduction, followed by a multivariate Gaussian fit that produces a stochastic model for keratoconus (SyntEyes KTC). The output of this model is filtered to remove the occasional incorrect topography patterns by either an automatic or manual procedure. Finally, the output of this keratoconus model is matched to that of the original model for normal eyes using the non-corneal biometry to obtain a description of keratoconus development.

Results: The synthetic data generated by the model were found to be significantly equal to the original data (non-parametric Mann–Whitney equivalence test; 145/154 passed). The variability of the synthetic data, however, was often significantly less than that of the original data, especially for the higher order Zernike terms of corneal elevation (non-parametric Levene test; $p < 0.05/154$). These results remained generally the same after applying either filter procedure to remove the synthetic eyes with incorrect topographies. Interpolation between matched pairs of normal and keratoconic SyntEyes appears to provide an adequate model for keratoconus progression.

Conclusion: The synthetic data provided by the proposed keratoconus model closely resembles actual clinical data and may be used for a range of research applications when (sufficient) real data is not available.

Introduction

In keratoconic eyes the cornea experiences a progressive conical deformation that gradually impedes the visual quality of the patient. Over the years many different optical methods have been proposed to correct for the optical aberrations induced by this condition, such toric spectacles, rigid gas-permeable contact lenses and scleral lenses.^{1,2} But while there is a great ongoing research interest in keratoconus correction, it is not always easy for investigators, especially those without clinical affiliations, to gain access

to patient data to test their solutions. For such research groups the use of keratoconic eye models may be a solution.

Although quite a few optical eye models have been proposed for normal eyes,³ far less work has been done on the optical modelling of keratoconus. The main contributions in this field were made by the Center for Laser Applications of the University of Tennessee Space Institute. They proposed using customised eye modelling as a means to reconstruct keratoconic retinoscopy patterns,^{4,5} and improved this later with an age-adjusted lens to reconstruct the root-

mean-square (RMS) of the ocular wavefront.⁶ Parallel to this approach they also proposed a procedure to fit a two-dimensional Gaussian distribution to the higher order Zernike coefficients of the anterior corneal elevation data in 54 patients with varying degrees of keratoconus. This distribution was then used to generate random Gaussian distortions, which were superimposed on anterior corneal surface of the Navarro eye model⁷ to investigate how the size and location of the corneal deformation influences refraction.⁸ Although very interesting, both models have their limitations as the customised model was only available for 16 patients, which may not be enough to include the wide variety in keratoconus geometry and severity known to exist. The Gaussian model, on the other hand, has the potential to deal with this wide variety, but may be too simple as it did not include the posterior corneal surface and anterior chamber depth, which are also affected by keratoconus. Furthermore, a single Gaussian function may not be enough to describe the more complicated surface elevation distortions typically found in advanced cases.

One last approach, proposed by González *et al.*⁹ is to build a multi-zone model of the cornea. Such a model does not consist of singular surfaces, however, but rather of a collection of discrete regions that each have their own refraction that would complicate its implementation in ray tracing software.

The aim of this paper is to present a keratoconic version of the previously published SyntEyes model, called SyntEyes KTC,¹⁰ capable of generating an unlimited number of random, but realistic biometry sets with the same statistical and epidemiological properties as the original data it is based on. This is essentially a combination of the customised approach by Chen *et al.*⁶ and the statistical approach by Tan *et al.*⁸ After verification, this is taken one step further by combining the SyntEyes models for normal and keratoconic eyes into a model describing the development of keratoconus over time.

Methods

Subjects

The keratoconic model presented is based on the data of 145 right eyes of 145 keratoconic patients recruited from the keratoconus consultation at the Antwerp University Hospital. These patients were aged 31.8 ± 9.8 years (range 17–60 years), predominantly male (70.3%) and of West-European ethnicity (95.2%). The stages of the disease was moderate to severe, with a mean spherical equivalent refractions of -4.69 ± 4.24 D (range -18.38 to $+1.63$ D), a mean cylinder of -3.5 ± 2.2 D (range -8.0 to -0.5 D), a mean keratometry of 43.19 ± 4.90 D (range 39.95–64.34 D), and a corrected visual acuity of 0.24 ± 0.26 logMAR ($\sim 6/10$ or 20/35 Snellen; range -0.18 to 0.98 logMAR, 6/4

to 6/60). Keratoconus was diagnosed based on a combination of typical clinical signs on a Scheimpflug topography (e.g. asymmetric bow tie pattern, conical protrusion near the corneal apex, skewed axes, etc.), along with symptoms seen with a slit lamp examination (e.g. Fleisher ring, Vogt striae, etc.). Exclusion criteria were prior ocular surgery, including crosslinking, and wearing rigid gas permeable (RGP) contact lenses less than one month before testing. Subjects were not dilated for their investigations, which could have had some minor influence on the biometric and wavefront readings in younger subjects.

This study was approved by the Ethical Committee of the Antwerp University Hospital and all subjects gave written informed consent prior to testing, in accordance with the Declaration of Helsinki.

Measurements and modelling

Each patient underwent a series biometry measurements to determine the refraction (ARK-700, Nidek, www.nidek.com), the anterior segment geometry (Pentacam HR, Oculus GmbH, <https://www.pentacam.de/en.html>), the lens thickness and axial length (Lenstar, Haag–Streit, www.haag-streit.com) and the ocular wavefront (eight orders over a 5 mm pupil diameter; iTrace, Tracey Technologies, www.traceytechnologies.com). This lead to a set of 97 biometric parameters (see Table 1 for an overview), which was reduced down to 18 by processing the corneal elevation Zernike coefficients using Principal Component Analysis (“eigencorneas”).¹¹ Next, these parameters were fitted with a linear combination of two multivariate Gaussian functions using Expectation–Maximization,¹² from which it is possible to generate an unlimited number of random biometry sets with the same distributions as the original data.^{10,13} Finally, these biometry sets (or SyntEyes) were filled in into the Navarro eye model⁷ to account for missing parameters, such as e.g. lens asphericity, that are difficult to obtain directly in a clinical setting. Given that it was recently demonstrated that keratoconic eyes only differ from normal eyes in their corneal shapes and anterior chamber depth,¹⁴ using lens parameters from a healthy eye model should not introduce any substantial errors. Once filled in, the model can be used to calculate the associated wavefronts, as well as the refraction in the form of spherical equivalent S.E., and Jackson power vectors J_0 and J_{45} .^{15,16} For a detailed overview of the parameters, conventions and methods used, we refer to our previous model for healthy eyes.¹⁰

Model of keratoconus development

By combining both the healthy¹⁰ and keratoconic eye models, it is also possible to come up with a description of how keratoconus develops from its earliest stages onwards. This description starts from a single keratoconic SyntEye and

Table 1. Comparison of the biometry of the keratoconic SyntEyes (1000 eyes) with the biometry of the original keratoconic data (145 eyes)

Parameter	Unit	SW*	Average (S.D.)		NPMWE†	NPL‡
			Original data	SyntEyes		
EC ₀	μm	0.14	−0.328 ± 77.924	2.701 ± 81.534	PASS	0.28
EC ₁	μm	0.009	−0.110 ± 40.459	−1.836 ± 42.423	PASS	0.52
EC ₂	μm	0.002	0.086 ± 30.475	−0.525 ± 32.556	PASS	0.61
EC ₃	μm	0.79	−0.002 ± 24.959	0.936 ± 25.702	PASS	0.72
EC ₄	μm	0.80	0.055 ± 15.100	−0.031 ± 14.457	PASS	0.73
EC ₅	μm	<0.001	−0.025 ± 9.632	0.340 ± 11.108	PASS	0.28
EC ₆	μm	<0.001	0.000 ± 7.897	0.119 ± 8.243	PASS	0.86
EC ₇	μm	<0.001	−0.005 ± 5.033	0.436 ± 5.710	PASS	0.45
EC ₈	μm	0.03	0.033 ± 4.761	−0.279 ± 5.306	PASS	0.69
EC ₉	μm	<0.001	−0.005 ± 4.390	−0.107 ± 4.334	PASS	0.35
EC ₁₀	μm	<0.001	0.000 ± 3.770	0.006 ± 3.688	PASS	0.91
EC ₁₁	μm	<0.001	0.001 ± 3.202	0.074 ± 3.504	PASS	0.04
ACD	mm	0.32	3.232 ± 0.354	3.225 ± 0.346	PASS	0.65
T	mm	0.13	3.759 ± 0.333	3.766 ± 0.323	PASS	0.13
L	mm	0.41	24.095 ± 1.063	24.141 ± 1.104	PASS	0.38
r _{La}	mm	0.19	11.327 ± 1.125	11.306 ± 1.111	PASS	0.98
r _{Lp}	mm	<0.001	−7.437 ± 0.707	−7.424 ± 0.699	PASS	0.37
P _L	D	0.001	22.714 ± 2.776	22.729 ± 2.734	PASS	0.017
CCT§	μm	0.05	498.41 ± 39.14	495.16 ± 42.23	PASS	0.46
Z _n ^m (CA)§	μm	45/45¶	–	–	All pass¶	24/45¶
Z _n ^m (CP)§	μm	45/45¶	–	–	All pass¶	27/45¶
Z _n ^m (WF)	μm	45/45¶	–	–	36/45 pass¶	35/45¶

SW, Shapiro-Wilk test for normality; NPMWE, non-parametric Mann–Whitney equivalence test, assuming uniform limits of tolerance and $\epsilon = 0.75$; NPL, Non-parametric Levene test for the equality of group variances; EC_i, eigencornea parameters; ACD, anterior chamber depth; T, lens thickness; L, axial length; r_{La}, r_{Lp}, anterior and posterior radius of the lens; P_L, lens power calculated using the Bennett equation; CCT, central corneal thickness; Z_n^m (CA), Z_n^m (CP), Z_n^m (WF), Zernike coefficients of anterior and posterior corneal elevation, and total ocular wavefront.

The full version of this table, including the influence of filtering, is available in Appendix S3.

* $p < 0.05$ (no Bonferroni correction applied) indicates a significant difference (in italics).

† $p > 0.05/154 = 3.25 \times 10^{-4}$ (Bonferroni correction) indicates a significant equality (in italics).

‡ $p < 0.05/154 = 3.25 \times 10^{-4}$ (Bonferroni correction) indicates a significant difference (in italics).

§Derived from eigencorneas EC₀...EC₁₁.

¶Number of comparisons with a significant result.

searches a large set of healthy SyntEyes for the one with values for lens power, lens thickness and vitreous depth close to those of the keratoconic SyntEye. This normal SyntEye will then serve as a proxy for the pre-keratoconus stage of the keratoconic eye. Modelling keratoconus development will then be a matter of interpolation between the normal and keratoconic states.

In real eyes the corneal deformation process in keratoconus typically starts between age 12–20 years and will continue to increase until it slows down to reach a certain end state. This course is reminiscent of the Gompertz function, a double exponential function of the form:

$$G(t) = \exp(-a \cdot \exp(-bt)) \quad (1)$$

that is sometimes used in myopia research for similar purposes.^{17,18} Fitting this function to real patient data is often not possible, however, as the biometry prior to

keratoconus onset is usually not available and the end state is rarely reached due to crosslinking treatment. For this reason studying the full natural progression of the disease is challenging. Furthermore, there is a wide range of possible variations in the keratoconus development, such as early or late onset, slow or rapid progression, and small or large end state deformation, which makes that choosing one uniform progression for all SyntEyes is not realistic. For this reason we assumed that all eyes will reach the end stage within 3–8 years, and that, like in myopia,^{17,18} Gompertz parameters a and b in this case are distributed according to a Beta distribution. For reasons of simplicity, age of onset, which is known to influence keratoconus progression speed, is not included in current model.

Once a suitable interpolation function $G(t)$ is available, the corneal shape parameters and the anterior chamber depth can be described as:

$$P(t) = P_N(t) + G(t) \cdot (P_K(t) - P_N(t)) \quad (2)$$

with P_N the parameters of the healthy SyntEye, and P_K the parameters of the keratoconic SyntEye. This is implemented as a Matlab program in Appendix S1.

Filtering the results

In practice we found that the topographies in 12–13% of keratoconic SyntEyes appear rather unkeratoconus-like, which we attributed to a combination of the extreme variations found in the original keratoconic data and non-linear interactions between eigencornea terms that could not be fully captured by the multivariate Gaussian model. Since such “odd” patterns may unacceptably influence any batch calculations performed with keratoconic SyntEyes, we developed two procedures that filter inappropriate patterns from the output. The first is fully automatic and works very fast and accurate, reducing the percentage of odd patterns to only 0.5%. It does, however, tend to also reject any correct pattern that deviates from the classical shape of an inferior steepening, such as superior or central keratoconus. The second procedure involves a visual inspection by the user, and is as such a more reliable, albeit much more labour-intensive, method of filtering. This allows preserving the rarer types of keratoconus. The results of the automatic and manual procedures are evaluated in Appendices S2 and S3; the results presented in the following are only for the unfiltered model output.

Statistics

Since almost all of the parameters considered in this work are not normally distributed according to the Shapiro-Wilk test (Table 1), often due to the presence of a small number of outliers, the use of non-parametric tests was required. The statistics in this work mostly involves demonstrating equivalence between the original data and the synthetic data, which is fundamentally different from an absence of a statistically significant difference as demonstrated by the standard difference testing. Instead a non-parametric Mann–Whitney test for equivalence (NPMWE) was used, which gives a binary *pass/fail* result. Further details on this test, as well as sample code, may be found in the book by Wellek.¹⁹ Differences in standard deviation between the original and synthetic data were demonstrated using a non-parametric Levene (or Brown-Forsythe) test.²⁰

All tests are performed at a confidence level of 0.05, adjusted with a Bonferroni correction in case of multiple simultaneous comparisons to avoid false positives. Following the recent recommendations by Armstrong²¹ this correction was applied to the NPMWE and the non-parametric Levene tests, since we are mostly interested in the overall equivalence of all parameters as a whole. Although there was interdependence between many of the parameters (suggested by Armstrong as a contraindication for a Bonferroni), we deemed the testing of the overall equivalence as more important in the context of this work.

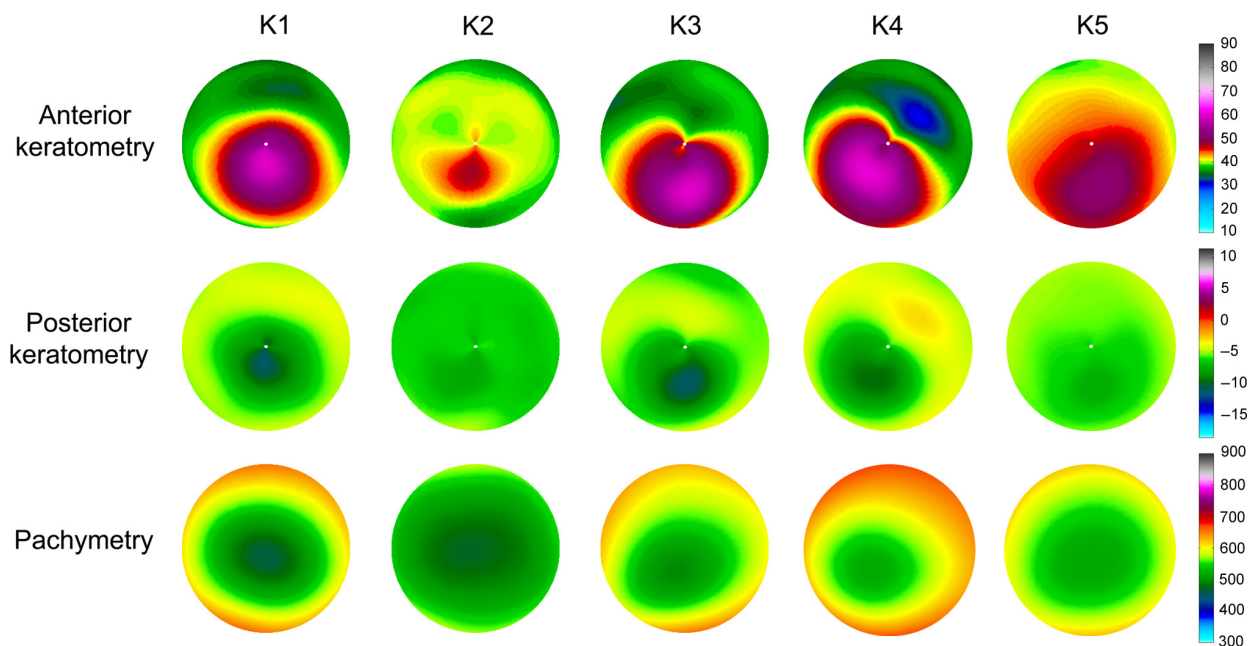


Figure 1. Five examples of keratoconic corneas generated by the model.

Bonferroni was not applied to the normality tests, as this may increase the chance of spurious fits by the model.²¹

Results

Verifications

The corneas generated by the model had keratometry maps closely resembling those of mid- to late-stage keratoconus, with clear protrusions on both the anterior and posterior surfaces, and thinning at the spot of greatest deformation (Figure 1). These synthetic corneas form the basis of current model.

The accuracy of the wavefront calculations was verified by comparing the wavefronts derived from the measured biometry to the originally measured wavefronts, and found them to be significantly equal (see figure in Appendix S3).

Comparing synthetic to original data

One thousand unfiltered keratoconic SyntEyes generated by the model were compared to the original data (Table 1). For all parameters considered the both datasets were found significantly equal to each other, with the exception of 9 wavefront Zernike coefficients of the 7th and 9th order (NPMWE, 145/154 passed). The distributions of the refractive components S.E., J_0 and J_{45} of the SyntEyes closely followed those of the original data as well (Figure 2). No differences in standard deviations between both datasets were seen for the 18 parameters used in the multivariate Gaussian fit (i.e. first 18 lines in Table 1). For the majority of the higher order Zernike coefficients, however, the standard deviations of the synthetic data was significantly smaller than that of the

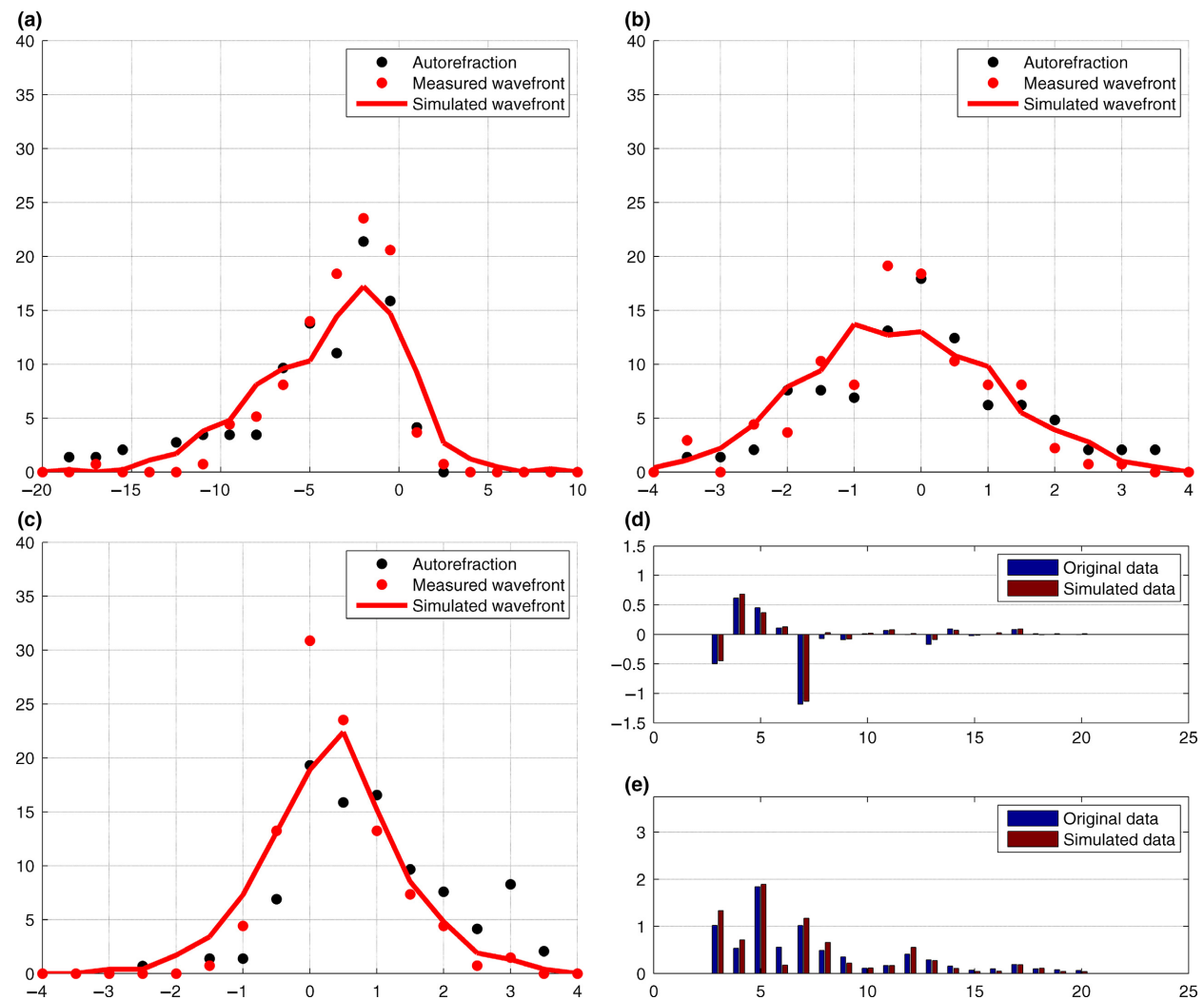


Figure 2. Verification of the refractive and wavefront results of the keratoconic SyntEyes model for (a) spherical equivalent, (b) Jackson cylinder J_0 , (c) Jackson cylinder J_{45} , (d) average and (e) standard deviation of the Zernike coefficients (8th order, Ø 5 mm; only first 20 coefficients are shown; mean and standard deviation of Z_2^0 (nr 5) divided by 5 for better visualisation).

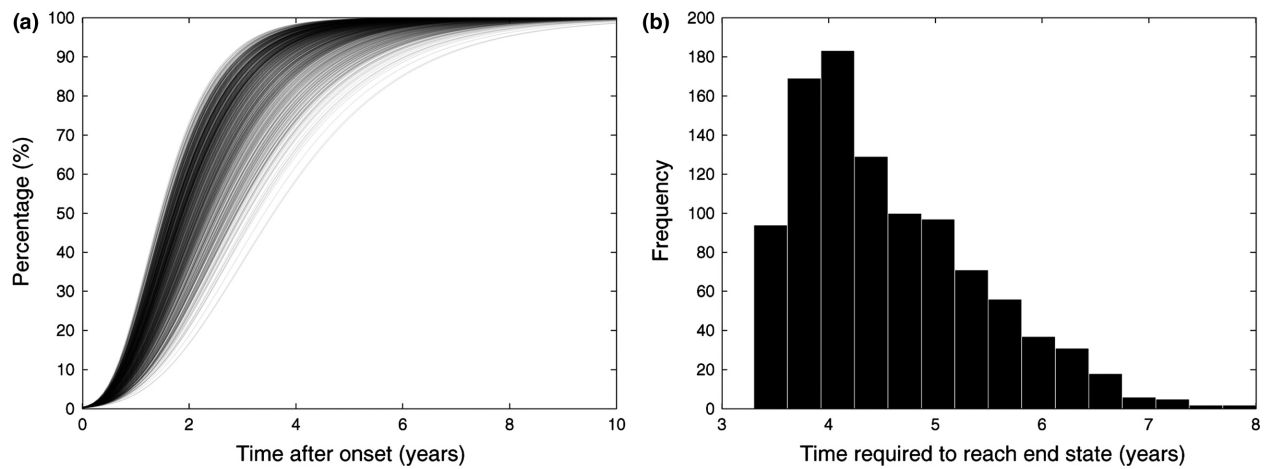


Figure 3. (a) Overview of 1000 Gompertz curves used for interpolation between normal and keratoconic SyntEyes with matching non-corneal biometry; (b) histogram of the time to reach 95% of the end stage (i.e. effective stabilisation of the cornea).

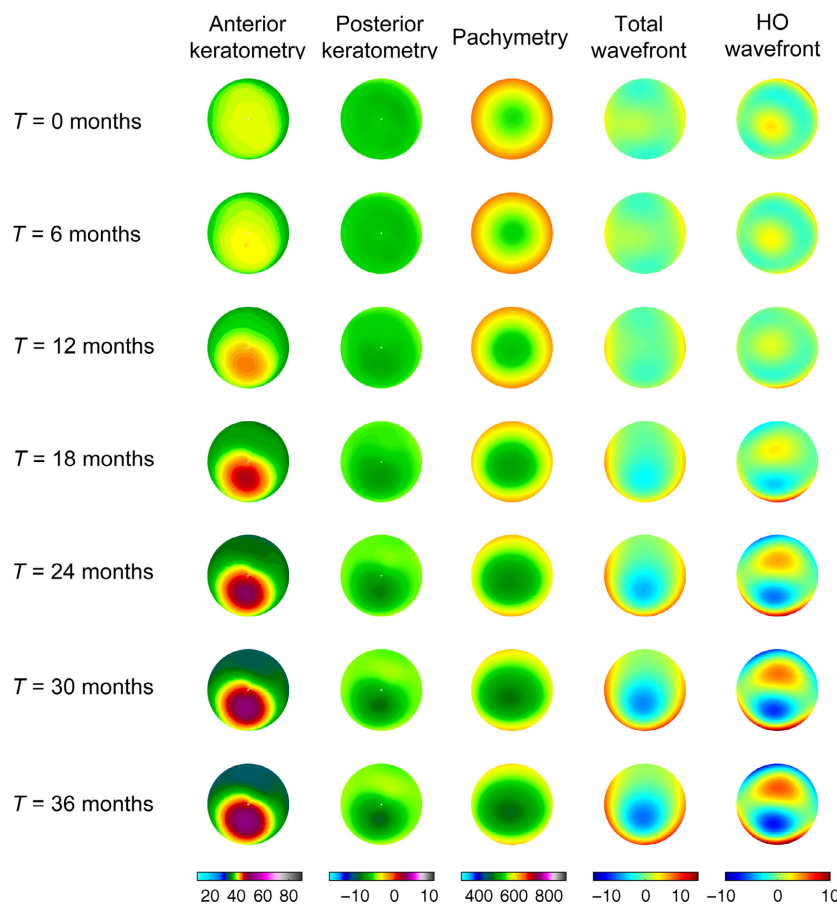


Figure 4. Example of developing keratoconus over a period of 3 years generated by the model, with a steadily increasing protrusion and thinning.

original data (F -test; $p < 0.05/154$). This was also seen in the model for normal eyes and was the result of using eigencorneas to reduce dimensionality.¹⁰

The results for manual filtering method showed very similar results as the unfiltered SyntEyes, but the automated filtering generally deviated further from the

original data than manual filtering (See Table SC1 in Appendix S3).

Note that the number of 1000 SyntEyes was chosen in order to obtain smoother curves. In order to check whether the number of SyntEyes used in the comparison played any role, we also performed a comparison of the original data with a set of 145 SyntEyes, which produced the same result.

Model of keratoconus development

In order to use Equation (2) for the interpolation between pre-keratoconic and manifest keratoconic eyes, suitable distributions for the Gompertz a and b parameters must be determined first. In practice we found that beta distributions $a = 5 + \text{Beta}(\alpha = 10; \beta = 3)$ and $b = 0.5 + \text{Beta}(\alpha = 4; \beta = 3)$ produced interpolation functions that reach the end stage within 3–8 years (Figure 3). Note that these beta distributions only represent an educated guess at best, since to the best of our knowledge there is no long-term follow-up data available in the literature by which these assumptions may be tested.

These distributions were used to generate random Gompertz curves to interpolate between pairs of normal and keratoconic SyntEyes, matched by their non-corneal biometry. An example of such a developing keratoconus is shown in Figure 4 and a sample of 1000 manually filtered SyntEyes, developing from normal ($T = 0$ months) to stabilised end-stage keratoconus ($T = 120$ months), is provided as Appendix S4.

Discussion

Like the earlier SyntEyes model for normal eyes, the keratoconic model produces an unlimited amount of synthetic biometry data that is a close approximation of actual biometry. To the best of our knowledge current keratoconus model is the most realistic one available in the literature, providing a wide variety of different keratoconus types that are also encountered clinically. As such, this is an interesting addition to the customised models by Chen *et al.*⁶ and the statistical approach with a single Gaussian distortion by Tan *et al.*⁸ As such, this model may be an interesting tool for researchers that do not have access to actual biometry data to develop new correction methods, e.g. in the form of customised spectacle or contact lenses. It may also assist in the development of a protocol to deal with the challenging intraocular lens power calculations in keratoconus patients. Combined with finite element modelling procedures available in the literature^{22–24} one could also obtain the SyntEyes' biomechanics and simulate the corrective effects of intrastromal rings.

Besides the 'static' keratoconus model, this work also presents a development model, which forms a powerful

tool to simulate e.g. how keratoconus progression affects optical or mechanical correction methods. This model is based on an Gompertz interpolation between pairs of keratoconic and normal SyntEyes, matched based on their non-corneal biometry. The matching process requires a large number of normal SyntEyes to be generated for each keratoconic SyntEye, ranging between 10^5 and 2.5×10^6 normal SyntEyes. Despite these large numbers, it can still occur that no match is found, at which point the keratoconic SyntEye is rejected and the algorithm moves on to the next one. Another method was considered to estimate the pre-keratoconic corneal shape for each keratoconic SyntEye. It fitted the elevation data of the corneal periphery of the current keratoconic shape, which should theoretically be less affected by the disease, to a corneal model.²⁵ This approach turned out to be unsuccessful, even in early KTC stages, as it would always reconstruct the central cornea into a keratoconic shape. Hence the current approach was chosen.

The synthetic data produced do have some limitations, however, most notably in the fact that the model does not add new information to what was already available in the original data and that the eigencornea procedure reduces parameter variability (see Table 1). These, and several other limitations, were already extensively discussed in the paper on the normal SyntEyes model.¹⁰ One issue specific to the current keratoconus model is that it also produces odd, non-keratoconic topography patterns in about 12–13% of SyntEyes it generates. This issue was dealt with using automatic or manual filtering procedure that produced similar results as either the unfiltered results or the original data. As the automated procedure leads to mean parameter values that deviate more from the original data than those of the manual procedure (77.3% of parameters significantly equal vs 94.2% for the automated and manual procedures, respectively; see Appendix S3), and that it tends to also reject rarer types of keratoconus, the authors prefer using the lengthier, but more accurate manual procedure.

Acknowledgements

The authors would like to thank Sien Jongenelen for her support in collecting the data. This project was supported by research grants by the Flemish government agency for Innovation by Science and Technology (grant nr. IWT/110684) and the Spanish Ministry of Economy and Competitiveness (FIS2014-58303-P).

Disclosure

The authors declare no competing interests.

References

- Romero-Jiménez M, Santodomingo-Rubido J & Wolffsohn JS. Keratoconus: a review. *Cont Lens Anterior Eye* 2010; 33: 157–166.
- Jhanji V, Sharma N & Vajpayee RB. Management of keratoconus: current scenario. *Br J Ophthalmol* 2011; 95: 1044–1050.
- Atchison DA & Thibos LN. Optical models of the human eye. *Clin Exp Optom* 2016; 99: 99–106.
- Chen Y-L, Tan B, Baker K et al. Simulation of keratoconus observation in photorefractive. *Opt Express* 2006; 14: 11477–11485.
- Tan B, Chen Y-L, Baker K et al. Simulation of realistic retinoscopic measurement. *Opt Express* 2007; 15: 2753–2761.
- Chen Y-L, Shi L, Lewis J & Wang M. Normal and diseased personal eye modeling using age-appropriate lens parameters. *Opt Express* 2012; 20: 12498–12507.
- Navarro R, Santamaria J & Bescós J. Accommodation-dependent model of the human eye with aspherics. *J Opt Soc Am (A)* 1985; 2: 1273–1280.
- Tan B, Baker K, Chen Y-L et al. How keratoconus influences optical performance of the eye. *J Vis* 2008; 8: 13.
- González L, Hernández-Matamoros JL & Navarro R. Multi-zone model for postsurgical corneas: analysis of standard and custom LASIK outcomes. *J Biomed Opt* 2008; 13: 044035-1 to 044035-12.
- Rozema JJ, Rodriguez P, Navarro R & Tassignon M-J. SyntEyes: a higher-order statistical eye model for healthy eyes. *Invest Ophthalmol Vis Sci* 2016; 57: 683–691.
- Rodríguez P, Navarro R & Rozema JJ. Eigencorneas: application of principal component analysis to corneal topography. *Ophthalmic Physiol Opt* 2014; 34: 667–677.
- Rozema JJ & Tassignon MJ. The bigaussian nature of ocular biometry. *Optom Vis Sci* 2014; 91: 713–722.
- Rozema JJ, Atchison DA & Tassignon M-J. Statistical eye model for normal eyes. *Invest Ophthalmol Vis Sci* 2011; 52: 4525–4533.
- Rozema JJ, Zakaria N, Hidalgo IR, Jongenelen S, Tassignon M-J & Koppen C. How abnormal is the noncorneal biometry of keratoconic eyes? *Cornea* 2016; 35: 860–865.
- Thibos LN & Horner D. Power vector analysis of the optical outcome of refractive surgery. *J Cataract Refract Surg* 2001; 27: 80–85.
- Thibos LN, Wheeler W & Horner D. Power vectors: an application of Fourier analysis to the description and statistical analysis of refractive error. *Optom Vis Sci* 1997; 74: 367–375.
- Thorn F, Gwiazda J & Held R. Myopia progression is specified by a double exponential growth function. *Optom Vis Sci* 2005; 82: E286.
- Flitcroft D. Emmetropisation and the aetiology of refractive errors. *Eye* 2014; 28: 169–179.
- Wellek S. *Testing Statistical Hypothesis of Equivalence and Noninferiority*. CRC Press: Boca Raton, 2010.
- Brown MB & Forsythe AB. Robust tests for the equality of variances. *J Am Stat Assoc* 1974; 69: 364–367.
- Armstrong RA. When to use the Bonferroni correction. *Ophthalmic Physiol Opt* 2014; 34: 502–508.
- Sinha Roy A & Dupps WJ. Patient-specific modeling of corneal refractive surgery outcomes and inverse estimation of elastic property changes. *J Biomech Eng* 2011; 133: 011002.
- Sinha Roy A & Dupps WJ. Patient-specific computational modeling of keratoconus progression and differential responses to collagen cross-linking. *Invest Ophthalmol Vis Sci* 2011; 52: 9174–9187.
- Simonini I & Pandolfi A. Customized finite element modelling of the human cornea. *PLoS One* 2015; 10: e0130426.
- Navarro R, González L & Hernández JL. Optics of the average normal cornea from general and canonical representations of its surface topography. *J Opt Soc Am A Opt Image Sci Vis* 2006; 23: 219–232.

Supporting Information

Additional Supporting Information may be found in the online version of this article:

Appendix S1. Matlab program to generate normal, keratoconic and developing keratoconic SyntEyes.

Appendix S2. Topographical analysis of the SyntEyes and filtering the output.

Appendix S3. Additional verification of the keratoconic SyntEyes model.

Appendix S4. Matlab file with the biometric and wavefront data of 1000 developing keratoconus SyntEyes.